# An S-Transform-based Technique for Shortening the Strong Motion Duration of Accelerograms for Rapid Time History Analysis

*Salar Arian-Moghaddam[1], Sayed Mohammad Motovali Emami[2*], and Mahmood Hosseini[3]*

1. Ph.D., Independent Researcher, Tehran, Iran
2. Assistant Professor, Department of Civil Engineering, Najafabad Branch, Islamic Azad University, Najafabad, Iran, *Corresponding Author; email: sm.emami@pci.iaun.ac.ir
3. Associate Professor, Structure Research Center, International Institute of Earthquake Engineering and Seismology (IIEES), Tehran, Iran

## ABSTRACT

*There are some cases, such as irregular or complex structures, in which the simplified analysis methods recommended by prevalent seismic codes are not able to yield results with acceptable precision. In such circumstances, the use of Non-Linear Time-History Analysis as the most robust response analysis approach is mandatory. This method is usually very time-consuming (mainly due to the small time steps). Therefore, any technique to reduce the computational cost, while keeping results in an acceptable range of precision, would be desired. There are some methods in the literature to increase the size of time step and simplify the recorded accelerograms by modifying time series. Although these methods may show negligible bias in results in terms of maximum response values of simple structures, they, definitely, impose some error due to the manipulation in the frequency content of the original signal. In this paper, an S-Transform based sim-plification procedure is introduced to overcome the drawbacks of available methods. The proposed method enables users to trace and compare the time-frequency variation of original and simplified signal to keep the general time-frequency pattern of signal and prevent the undesired omissions of components. Eleven strong ground motion records were selected to be used in the efficiency evaluation of the proposed method. The results of analyses for a range of single and multi-degree of freedom non-linear dynamic systems confirm the ability of shortened records to represent their original counterparts in terms of response characteristics. The results show that by a reduction of 71% in the analysis cost, the maximum observed error in the estimation of collapse of MDOF structures will be lower than 10%.*

## 1. Introduction

In seismic evaluation and design of structures, there are several cases in which the simplified seismic analysis procedures suggested by design codes, are not applicable. In such cases as irregular buildings, tall buildings and many special structures or critical facilities, most seismic codes recommend Time History Analysis (THA). THA can be very time-consuming, especially, when user needs to estimate collapse capacity of target structure, where Non-Linear Time-History Analysis (NLTHA) becomes necessary.

The idea of accelerogram simplification is not

new in earthquake engineering [1]; however, recently and coincidentally with increase in application of NLTHA, some researchers have tried to develop efficient methods to overcome limitations of simplification. Another available method is to define significant duration of ground motion and shorten the accelerogram such that the criteria controlling response parameters are satisfied [2]. The existing studies focus on the decrease of computational time without losing much precision. One approach suggests the application of larger time steps using different algorithms proposed by some researchers like Soroushian [3], Hosseini and Mirzaei [4], Faroughi and Hosseini [5], Basim and Estekanchi [6], Cheng et al. [7] and Soroushian [8]. Main shortcoming of these methods is related to the disturbance in the frequency content of the original signal [9-11]. The superiority of the application of "effective duration" is due to the preservation of original frequency content of ground motion in the remained significant duration [12-13]

Although attempts of researchers to reduce the required time for NLTHA have been basically successful, still the errors imposed to the response calculation, mainly due to the partial omission of high frequencies, is a discouraging factor in using the proposed techniques, particularly in case of low period structures [14-15]. Therefore, any method which can reduce the level of imposed error is still desired. This study is an effort to reach the mentioned goal, based on the S-transform, which makes it possible to combine the advantages of Short Time Fourier Transform (*STFT*) and Wavelet Transform (*WT*), as two main methods in the family of Time-Frequency Representation (*TFR*) techniques.

As the suggested method is based on the *TFR*, in this part of the paper at first a brief review is done on the general TFR approach and its background. Then the proposed S-transform method is explained in details, and finally its efficiency is shown by presenting some numerical examples covering both SDOF and MDOF systems.

Time-Frequency Representations (TFRs): Earthquake ground motions are known to have non-stationery nature, both in their amplitude and frequency content [16]. The problem of the inability of conventional spectral analysis using Fourier transform to describe the evolutionary spectral characteristics of non-stationary processes can be solved by using time-frequency spectral analysis [17]. One of the first TFRs providing required localization in time and frequency to establish a local spectrum for any time instant is *STFT* [17]. STFT applies Fourier transform to the signal after it is multiplied by a narrow window cantered at a time *t*. This window is shifted in time domain to obtain the local frequency content at any time instant. The resolution of *STFT*, which is defined as the capability of a transform to capture the short duration variations in the time and frequency domain, is dependent directly on the properties of the window used in time-frequency analysis [17]. In other words, a short window is required to ensure acceptable time resolution and a wider one to provide good frequency resolution. That the high resolution cannot be attained in both the time and frequency domain simultaneously is the main drawback of *STFT* [17]. Readers are referred to [17] for more details on the mathematical formulation. *STFT* of a signal such as is given by:

$$STFT(\tau, f) = \int_{-\infty}^{\infty} x(t)w(t-\tau)e^{-i2\pi ft}dt \qquad (1)$$

where $\tau$ denotes the location of time window and *f* is the frequency of interest, *w* represents the time window function and *X* denotes the time series as a function of time (*t*). The explained shortcoming of *STFT* can be tackled using multi-resolutional techniques based on *WT*, which uses a basis function that dilates and contracts with frequency [18]. In fact, the time-frequency window can change automatically to analyze the high-frequency contents of a signal as well as low-frequency components that offers better resolution. The continuous wavelet transform of a square integrable function, such as, can be calculated as:

$$WT(a, b) = \int_{-\infty}^{\infty} y(t)\psi_{a,b}^{*}(t)dt \qquad (2)$$

where *a* is the parameter controlling the dilation and contraction, *b* denotes the translation parameter, *y* denotes the time series as a function of time (*t*) and the asterisk represents the complex conjugate of the selected mother wavelet given as:

$$\psi_{a,b}^{*} = \frac{1}{\sqrt{|a|}}\psi\left(\frac{t-b}{a}\right) \qquad (3)$$

More detailed information on the mathematical calculation of *WT* can be found in [19]. *WT* cannot assess the local phase information. Moreover, the interpretation of results of wavelet analysis requires the knowledge of the details of the mother wavelet and is difficult for visual analysis. Stockwell et al. [20] have proposed a time-frequency representation called 'S-Transform', which can be considered as the extension of *STFT* and *WT*. Hence, one can describe the S-Transform as a frequency dependent *STFT* or a phase corrected *WT* that is [17]:

$$ST\left(f,\tau\right)=\int_{-\infty}^{\infty}x(t)g(t-\tau)e^{-i2\pi ft}dt \tag{4}$$

where, *g* represents the Gaussian time window function. Recently, a band variable filter having the ability of acting simultaneously in frequency and time domain has been applied to the analysis of non-linear dynamic behaviour of soil and buildings [6-7]. Also, Ghodrati Amiri and Arian-Moghaddam [21], Hasan and Kim [22], Bajaj and Kumar [23] and Latfaoui and Reguig [24] have proposed the S-Transform-based signal decomposition technique to extract velocity pulses of near fault ground motions.

S-Transform based filtering of time series [25] and the generations of synthetic accelerograms have been examined by some researchers [26-27]. The readers are referred to [18-20] for detailed information describing the formulation of S-Transform analysis.

## 2. The Proposed Method

Here, the suggested filtering approach in [28-31] is used to monitor the time frequency variation of input signal and extract the target part (also called shortened or filtered signal). Following the described necessity to the reduction of the computational time of analysis, in the previous section, the main goal of this work is to propose a shortened accelerogram such that the disorderliness in the time variation of frequency content is minimized. Therefore, it is tried to simplify the input signal by reduction of the duration and simultaneously keeping the response characteristic in an acceptable tolerance compared to those obtained by using the original accelerogram. Because of the merits of the S-Transform, it was selected as the TFR used in the filtering procedure in this study. There is sufficient scientific evidence confirming the superiority of the S-Transform

compared to other alternatives [21]. The general steps of the method can be summarized as:

❖ Run the TFR analysis of accelerogram by using S-Transform.

❖ Find the most severe (showing the largest amplitude values based on the Equation (4)) region in time-frequency domain.

❖ Define a quantitative (based on normalized ratio of amplitude, for example) or qualitative (by visual judgment) criterion to select the target parts of the original signal and extract the desired portion.

❖ Reconstruct the shortened signal in time domain by computing the inverse transform of the extracted signals in the previous steps.

Figure (1-a) in the next section of the paper shows the time-frequency variation of a sample
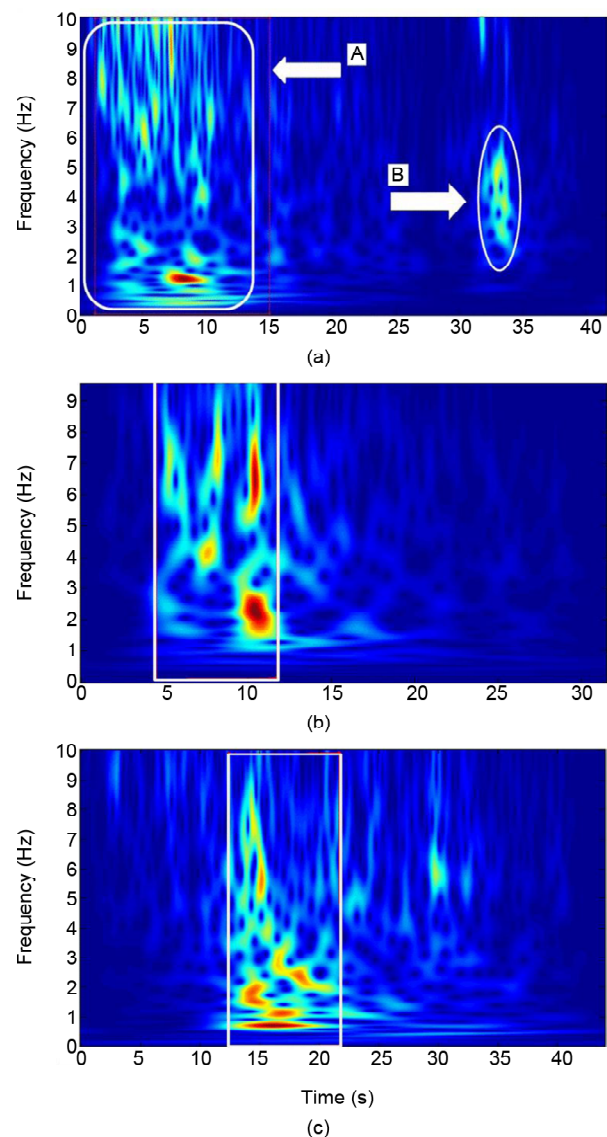


**Figure 1.** Time-frequency variation of the three sample records; R1 (a), R2 (b) and R3 (c).

acceleration time history. It should be mentioned that part B in the figure, as the second remarkable part of the time-frequency representation of the record, can be omitted since its frequency content is basically included in part A.

It is worth mentioning that, generally, there is a possibility to use a predefined intensity measure (IM), for example absolute or relative absorbed energy [32] to check the precision of the result and repeat the whole steps so as to satisfy the threshold criteria. It should be noted that although there are many definitions of strong motion duration in the literature [2], none of them allows a drastic reduction in duration as much as the reduction gained by the presented method in this study. Furthermore, it is possible to combine other simplification methods, such as increased time step size [3], with current duration reduction method, while it is not in the scope of present study. To show the efficiency of the proposed record simplification method some numerical examples are presented in the following

section.

Figure (1) shows the time-frequency variations of the original records, and Figure (2) compares the record pairs in time domain.

Comparing the values in Table (1) indicates that in case of each ground motion parameter there is a difference between original and shortened record. These differences are more in case of R3 (Chi-Chi earthquake) than two other records. To better investigate the effect of shortening the elastic and inelastic response spectra of both original and shortened records were computed in MATLAB programming environment [33], considering a damping ratio of 5% and 'constant-ductility' [34] factor of $\mu = 4$. The developed spectra are shown in Figures (3) to (5). It should be noted that the details of numerical method used to develop the response spectra can be found in [35].

It is observed in Figure (3) that there is a good match between the spectra of original and shortened record pair R1, while in case of record pair R2 there
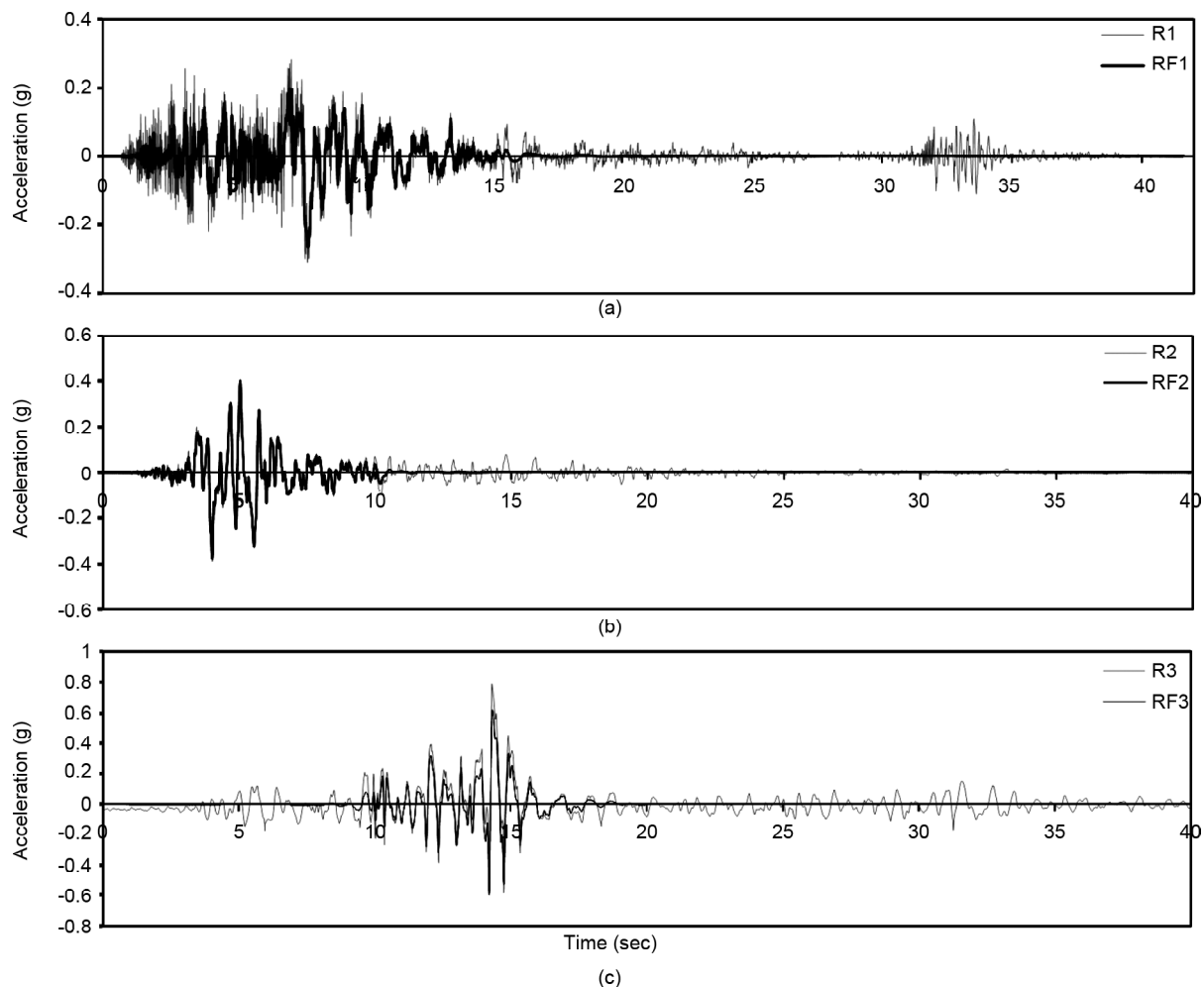


**Figure 2.** Time-frequency variation of the three sample records; R1 (a), R2 (b) and R3 (c).

**Table 1.** General features of records used in this study.

| No. | Event | Label | Year | $M_w$ | PGA (g) | PGV (cm/s) | PGV/PGA (sec) | Duration (sec) | AI* (m/s) | CAV** (cm/s) |
|-----|-------|-------|------|-------|---------|------------|---------------|----------------|-----------|--------------|
| 1 | Imperial Valley | R1 | 1979 | 6.5 | 0.311 | 53.79 | 0.176 | 40.8 | 1.57 | 1140 |
|   |                 | RF1 |      |     | 0.266 | 48.5 | 0.186 | 16 | 0.894 | 666 |
| 2 | Loma Prieta | R2 | 1989 | 6.9 | 0.406 | 45.655 | 0.115 | 39.8 | 1.51 | 890 |
|   |             | RF2 |      |     | 0.399 | 37.1 | 0.095 | 10 | 1.267 | 559 |
| 3 | Chi-Chi | R3 | 1999 | 7.6 | 0.786 | 258.9 | 0.336 | 40 | 5.47 | 2214 |
|   |         | RF3 |      |     | 0.623 | 70.2 | 0.11 | 10 | 3.1 | 965 |

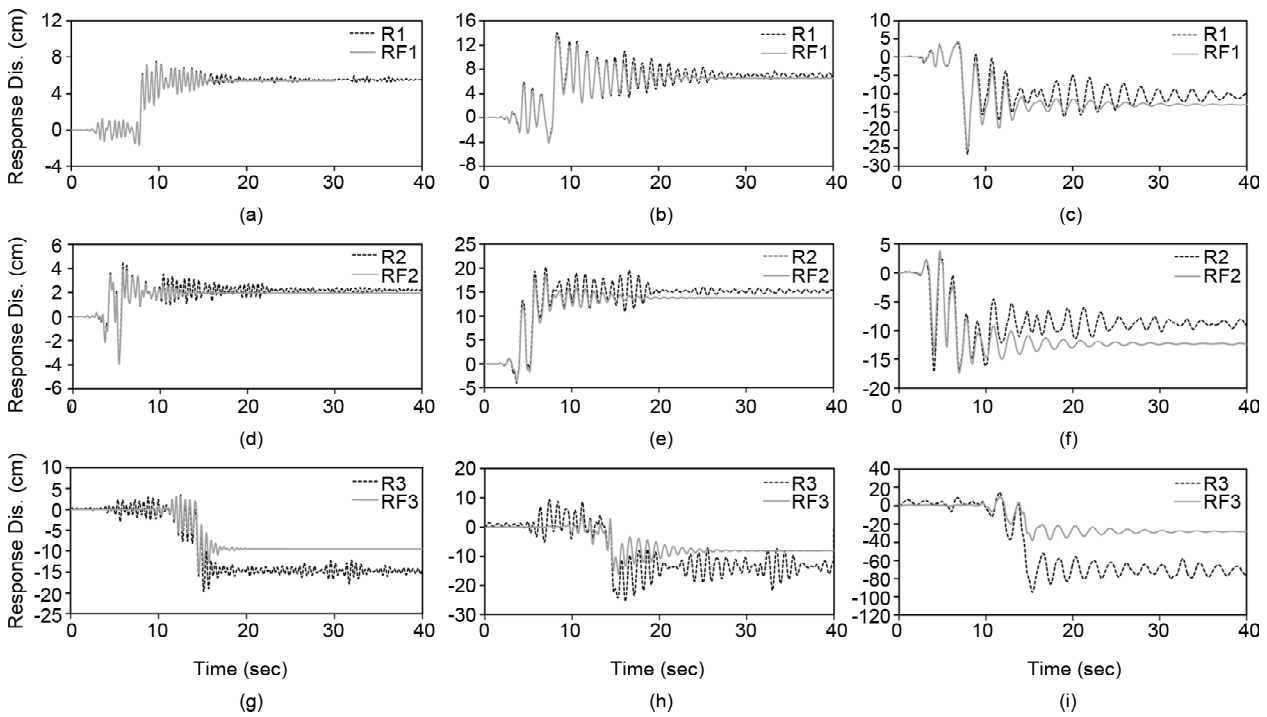* Arias Intensity [36]
** Cumulative Absolute Velocity [36]
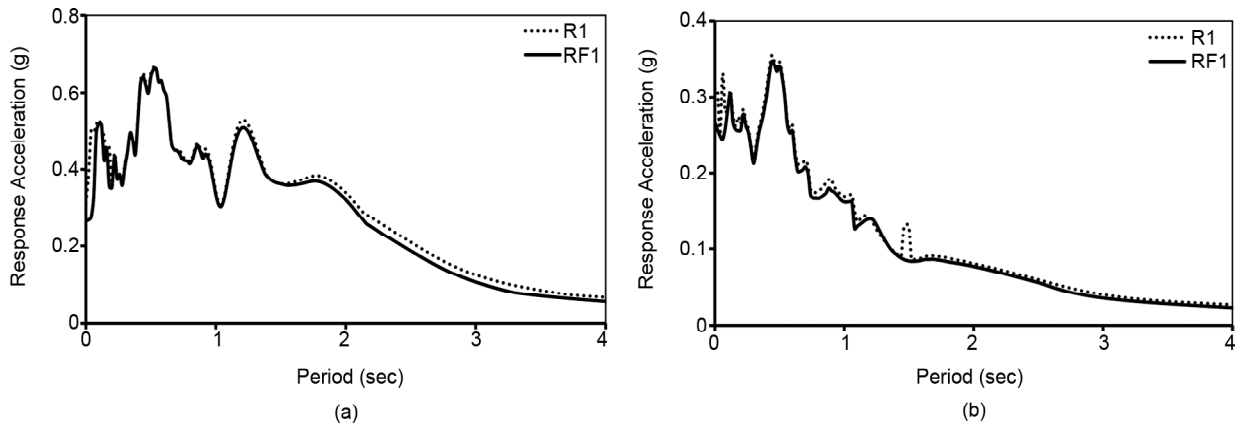


**Figure 3.** (a) Elastic and (b) inelastic response spectra of original and shortened record pair R1.
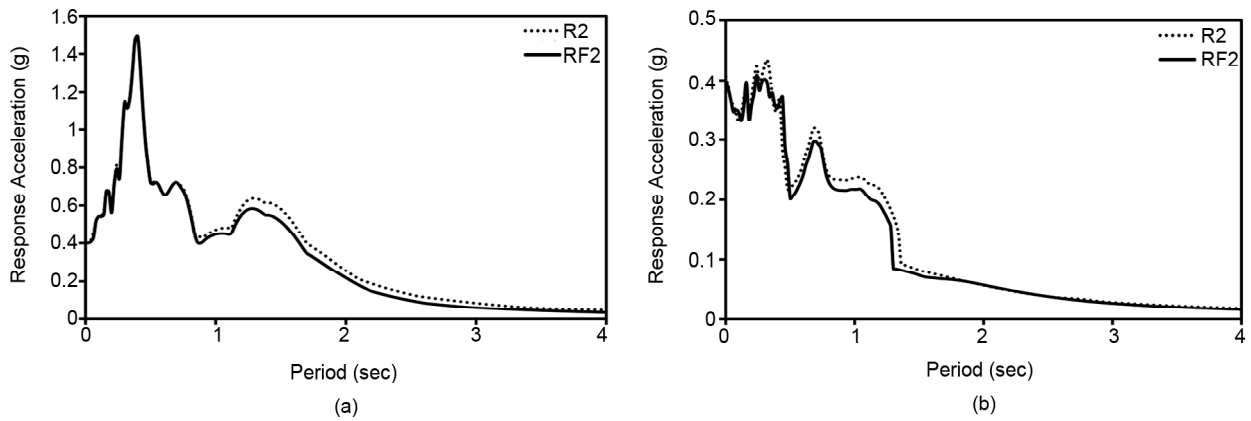


**Figure 4.** (a) Elastic and (b) inelastic response spectra of original and shortened record pair R2.
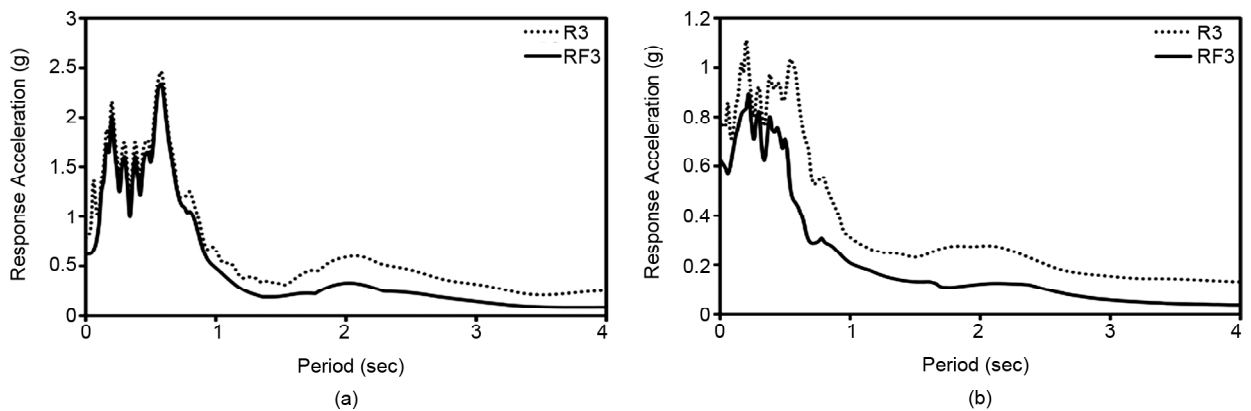


**Figure 5.** (a) Elastic and (b) inelastic response spectra of original and shortened record pair R3.

**Figure 6.** Response histories of inelastic SDOF systems with various period (T) subjected to record pair R1: (a), (b) and (c); Record pair R2: (d), (e) and (f); record pair R3: (g), (h) and (i) for T = 0.5s ,T = 1 and T = 2s, respectively (inelastic response have been calculated by assuming μ = 4).

is slight difference between the two spectra, as shown in Figure (4), and this difference is somehow remarkable in case of record pair R3 as shown in Figure (5). To see if the observed differences are only in the peak response values, given by the spectra, or they are also observed in the whole response histories, displacement response histories of SDOF systems having fundamental periods of 0.5, 1.0 and 2.0 sec with 5% damping were calculated under seismic excitations in Figure (6).

Good agreement between time history responses in shortened duration (0 to 16 sec) of the excitation corresponding to record pair R1 can be observed in Figure (6a-6c). The difference between response histories after the 16th sec till the end instant of the original record can be attributed to the fact that the response under shortened record after the 16th sec is actually only free vibration response. With regard to record pair R2, as shown in Figure (6d-6f), a more distinct difference is observed after the 10th sec, the cut instant; however, the maximum responses, which have occurred in the 7th sec, are in good agreement. This is while in case of record pair R3, as shown in Figure (6g-6i), the difference in the peak response values are not negligible any more, and this is due to extensive

shortening of the original record, resulting in loss of a relatively large portion of its total input energy as can be observed clearly in Figure (7).

As it is seen in Figure (7), in case of record R3 around 15% of the total energy of the record has been lost due to shortening, while in case of the records R1 and R2, almost the main part of the record energy has been kept during the shortening process.
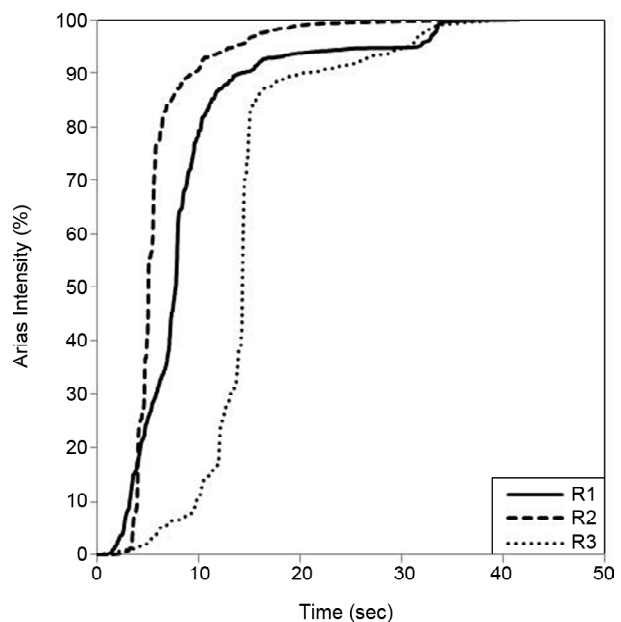


**Figure 7.** Energy flux of the three used original records.

One remedy for compensation of the lost energy in the shortened record would be linear amplitude scaling. However, this scaling is only reasonable if the frequency content of the deleted parts of the original record do not differ drastically from the kept part (the shortened record). Figure (8) shows the time-frequency variation of the deleted parts of record R3.

To see how effective is the proposed shortening technique in decreasing the duration of records, the original and shortened durations of the three selected sample records, introduced in Table (1), are compared in Table (2).
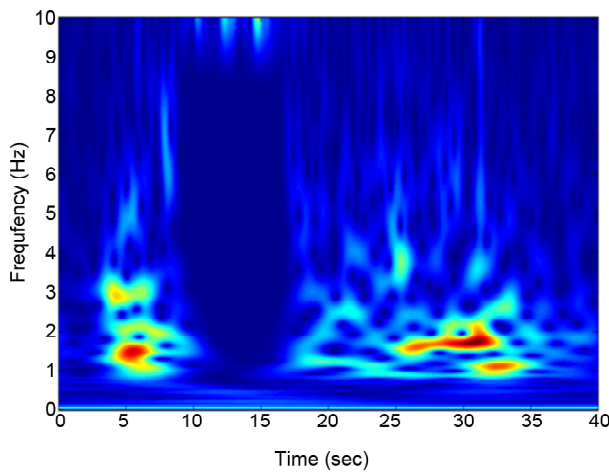


**Figure 8.** Time-frequency variation of the deleted parts of the record R3.

**Table 2.** Computed durations based on different definitions [37].

| Case | Duration (sec) | | |
|:---:|:---:|:---:|:---:|
| | **Significant** | **Uniform** | **Effective** |
| R1 | 29.1 | 17 | 35.4 |
| RF1 | 8.48 | 10.96 | 14.48 |
| R2 | 10.1 | 10.9 | 22.5 |
| RF2 | 3.93 | 5.95 | 8.38 |
| R3 | 24.4 | 18.1 | 37.9 |
| RF3 | 4.2 | 6.38 | 8.4 |

To have a more legible justification between response characteristics of input and output signals, readers should keep in mind that the shortened record consists of some real components of original record which are not scaled. It can be seen in Table (1) that the peak values of strong ground motions the shortened records are not the same as the original ones. In coming sections, a brief discussion about the possible role of scaling in alleviation of the observed differences is presented.

## 3. The Role of Scaling Shortened Records in Improvement of the Results

It was shown in the previous section that success of the proposed method is questioned in some cases such as record pair R3. Although the observed differences in the results of structural analyses by using the shortened records can be attributed to the omission of some frequencies of the excitations, it should be emphasized that the shortened records have not been scaled to any predetermined value. In other words, since the peak ground values of shortened accelerogram differ to some extent from those of the original one their corresponding response will not be quite similar as well. However, it is possible to reduce the difference in the results by applying a suitable scaling procedure. Figure (9) depicts the spectral ratio calculated for original and shortened record of Chi-Chi event (the worst case based on response characteristics) based on using Equation (5):

$$S_r = \frac{PSV_{oroginal}}{PSV_{shortened}} \tag{5}$$

Although this ratio, as shown in Figure (6), is not constant for all natural periods, one can recognize
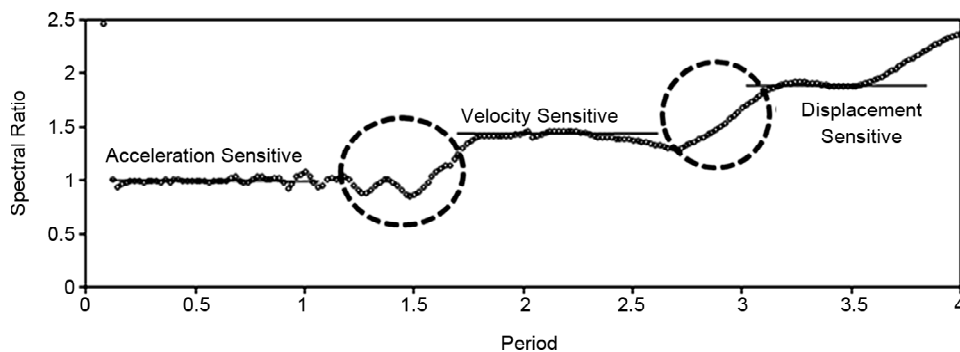


**Figure 9.** Spectral ratio computed for Chi-Chi original and shortened accelerograms.

three distinct regions at which a constant value can be assumed for that. These regions can roughly considered as acceleration-, velocity-, and displacement-sensitive corresponding to the structures with short, moderate and long natural periods, respectively. This fact enables users to define an appropriate scale factor such that ensures spectral consistency in the period range around the predominant period of the target structure. Figure (10) shows the acceleration response spectrum of original and shortened accelerograms after being scaled to a sample target spectrum at a natural period of 2.5s. Figure (11) compares response histories in elastic and inelastic states for the record pair R3, and Table (3) compares their basic characteristics after scaling.

## 4. Efficiency of the Shortened Records in MDOF Systems

To investigate the efficiency of the proposed method in case of MDOF systems response analysis, three 2-D steel moment resistant frames (MRF) were modeled by OpenSees [37] finite element program; including a 3-story frame representing

**Table 3.** Evaluation of results after scaling.

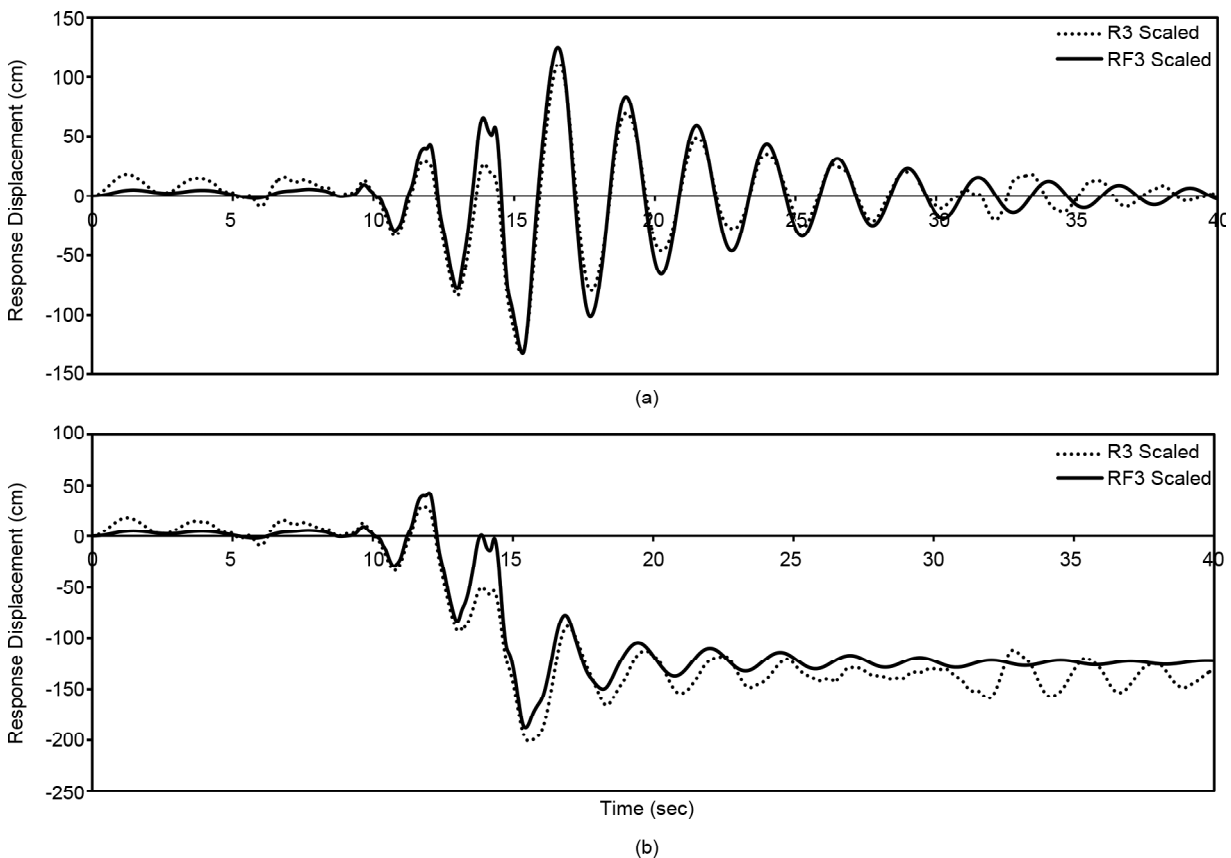| Scaled | HI[*] (cm) | CAV (cm/s) | Tp[**] (sec) | Tm[***] (sec) |
|---|---|---|---|---|
| R3 | 560.9 | 4135 | 0.58 | 0.68 |
| RF3 | 751.34 | 3590 | 0.58 | 0.57 |

[*] Housner Intensity [33]
[**] Predominant Period [33]
[***] Mean Period [33]
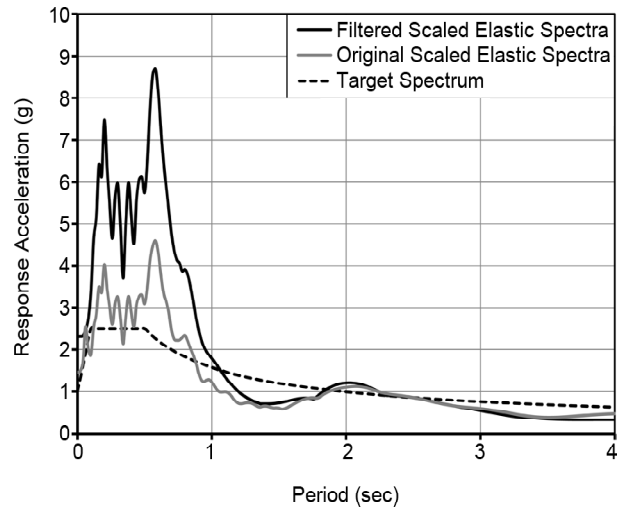


**Figure 10.** Acceleration response spectra of record pair R3 scaled to the target spectrum at T=2.5 spectral ratio computed for Chi-Chi original and shortened accelerograms.



(a)



(b)

**Figure 11.** (a) Chi-Chi elastic response history (b) Chi-Chi inelastic response history, for SDOF with T = 2.5s and μ = 4.

structures with short period of vibration, a 6-story frame, which belongs to the typical medium range of natural period of vibration and a 12-story frame as the representative of flexible long period structures. These frames were selected from a large database of structural systems introduced in [38], which are originally used to predict the structural displacements under seismic excitation. A gravity load on the beams equal to 27.5 KN/m (dead plus live loads) was considered. Table (4) presents general characteristics of the structural models as well as their dynamic modal properties. More information about the used structural systems can be found in [39].

Incremental dynamic analyses (IDA) [40] were carried out to evaluate the ability of the proposed method in prediction of the seismic behavior of nonlinear MDOF systems. Sixteen accelerograms were selected from [41] to cover a range of moment magnitude from 6.5 to 7.3, while the original recorded duration of ground motions were more than 30 seconds in all cases. The general features of the selected ground motions are presented in Table (5). Intensity levels were controlled at each step by scaling up the spectral response at first mode of vibration (Sa-T1) to a predefined value. The range of used scale factor started from 0.1g and was increased by steps equal to 0.1g until the maximum inter-story drift ratio of 0.2 was observed or structural instability occurred.

**Table 4.** Details of the structural models used in this study.

| Story | Bay | Column: (IPB) - Beams: (IPE) | Period (sec) | | |
|---|---|---|---|---|---|
| | | | Mode 1 | Mode 2 | Mode 3 |
| 3 | 3 | 260-330(1-3) | 0.65 | 0.19 | 0.11 |
| 6 | 3 | 300-360(1-4)+280-330(5-6) | 1.13 | 0.37 | 0.2 |
| 12 | 3 | 450-360(1)+450-400(2-3)+450-450(4-5)+400-450(6-7)+360-400(8-9)+360-360(10)+ 360-330(11-12) | 1.67 | 0.59 | 0.33 |

**Table 5.** Selected ground motion for IDA.

| No. | Earthquake | Station | PGA (g) | PGV (cm/s) | Moment Magnitude | Closest Distance to Rupture (km) | Duration (s) | | |
|---|---|---|---|---|---|---|---|---|---|
| | | | | | | | Significant 5-95% | Effective | Recorded |
| 1 | Northridge | 90091 LA - Saturn St. | 0.474 | 34.6 | 6.7 | 30 | 11.53 | 8.74 | 31.56 |
| 2 | Northridge | 24538 Santa Monica City Hall | 0.883 | 41.7 | 6.7 | 27.6 | 8.76 | 9.82 | 39.94 |
| 3 | Duzce, Turkey | Bolu | 0.822 | 62.1 | 7.1 | 17.6 | 9.35 | 12.51 | 55.87 |
| 4 | Imperial Valley | 6605 Delta | 0.351 | 33 | 6.5 | 43.6 | 50.33 | 60.45 | 99.89 |
| 5 | Kobe | 0 Kakogawa | 0.345 | 27.6 | 6.9 | 26.4 | 12.86 | 11.44 | 40.93 |
| 6 | Landers | 22074 Yermo Fire Station | 0.245 | 51.5 | 7.3 | 24.9 | 17.62 | 16.6 | 43.94 |
| 7 | Landers | 22170 Joshua Tree | 0.284 | 43.2 | 7.3 | 11.6 | 26.08 | 28.7 | 43.94 |
| 8 | Loma Prieta | 47524 Hollister - South & Pine | 0.371 | 62.4 | 6.9 | 28.8 | 16.395 | 17.91 | 59.94 |
| 9 | Bam | Bam | 0.777 | 109.9 | 6.2 | 1.7 | 7.66 | 7.69 | 24 |
| 10 | Tabas | Tabas 9101 | 0.85 | 117.46 | 7.4 | 2.5 | 15.68 | 15.78 | 24 |
| 11 | Tabas | Deyhook- 1082 | 0.334 | 27.69 | 7.3 | 9.0 | 0 | 31.76 | 40 |
| 12 | Tabas | TBS-A-1084 | 0.93 | 119.19 | 7.4 | 9.0 | 2 | 16.59 | 28 |
| 13 | Chalan Choolan | CHL-4027 | 0.44 | 46.23 | 6.1 | 6 | 1 | 11.64 | 26 |
| 14 | Ab-bar | ABB-A-1362 | 0.65 | 65.74 | 7.3 | 12 | 17 | 28.32 | 42 |
| 15 | Satarkhan Dam | SAT3-5588 | 0.24 | 29.77 | 6.4 | 7 | 6 | 15.1 | 38 |
| 16 | Zarand | ZRN-3671 | 0.29 | 26.30 | 6.4 | 7 | 13 | 16.97 | 40 |

## 5. Numerical Illustration in Terms of IDA Results

Results of IDA analyses are depicted in Figure (10) for the three steel MRFs, and Figures (12) and (13), compares the mean IDA curves for two the sets of original and shortened ground motions.

As it is clear in Figure (12), after the reduction of duration, the mean IDA curve can be estimated with acceptable precision, while the accuracy of approximation is much more in case of 6-story frame. On this basis, one can conclude that the nonlinear capacity of stiff structures is overestimated by using the shortened records, in a similar manner for more flexible systems (12-story frame), the precision of the proposed method may slightly decay. Therefore, the application of the duration reduction would be

more efficient, in case of medium rise structures when the dynamic behavior is not severely sensitive to the stiffness or mass of structures. In other words, a precise estimation is possible for structures which are located in the velocity controlled region of response spectra. It should be noted that in the mention region the seismic behavior of structure is mainly sensitive to the damping.

The deviation of IDA curves for shortened ground motions from exact prediction starts simultaneously with the initiation of structural softening due to the nonlinear behavior. It should be noted that the success of the proposed method is directly dependent on the level of imposed manipulation on the frequency content of ground motion. Fortunately, this can be measured using any conventional spectral analysis such as Fourier analysis.
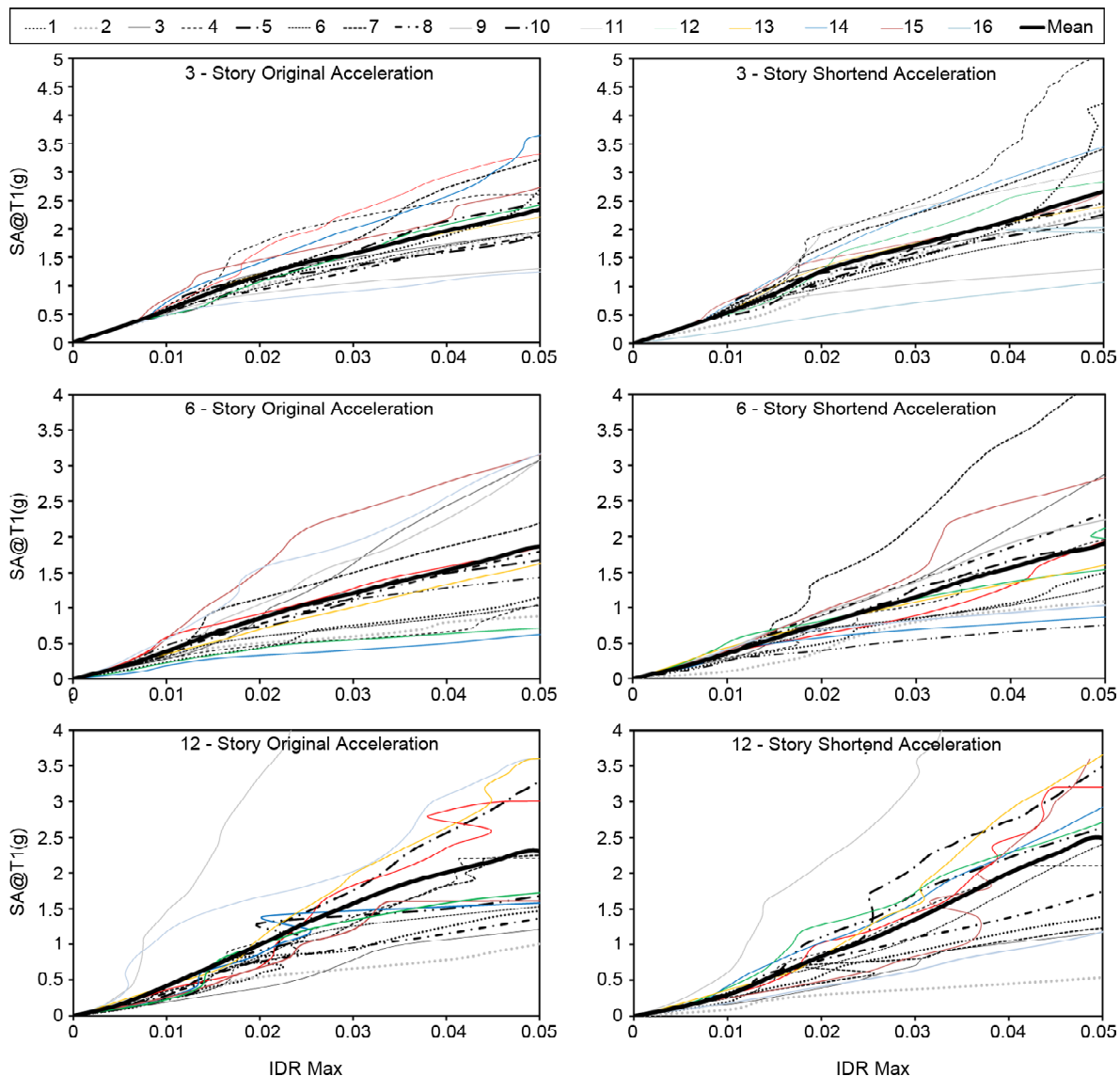


**Figure 12.** Results of the considered fame structures for the eight selected ground motions.

To evaluate the potential ability of a shortened ground motion in representing the original ground motion, the elastic acceleration response spectrum for 5% damping ratio was computed for each shortened ground motion and was normalized to the same value calculated for original one, defined as "Spectral Ratio". It should be noted that all ground motion must be scaled such that the same Sa-T1 be observed for each structural system. In this way, one can compare efficiency of method under the effect of both higher modes of vibration (natural periods lower than $T_1$) and structural softening (natural periods longer than $T_1$). Figure (14) shows the Spectral Ratios computed for different frames.

As Figure (12) depicts, ground motion No. 2 and No.16 show a completely different trend in the

whole period range, while other 14 shortened ground motions can represent the corresponding original signals at periods shorter than $T_1$; however, they underestimate the spectral values at period longer
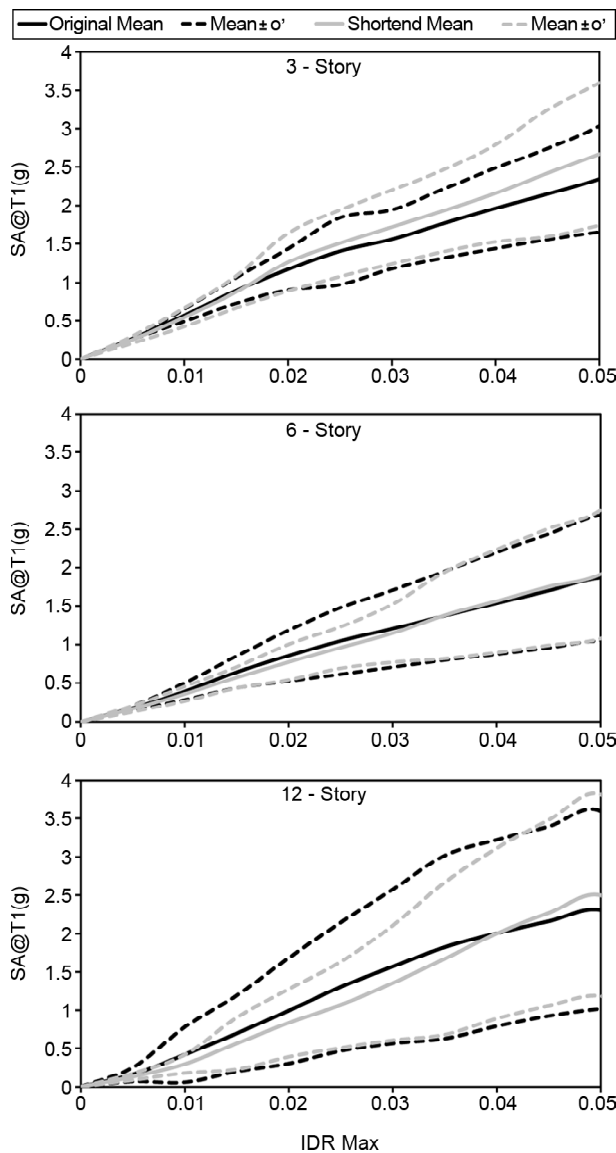


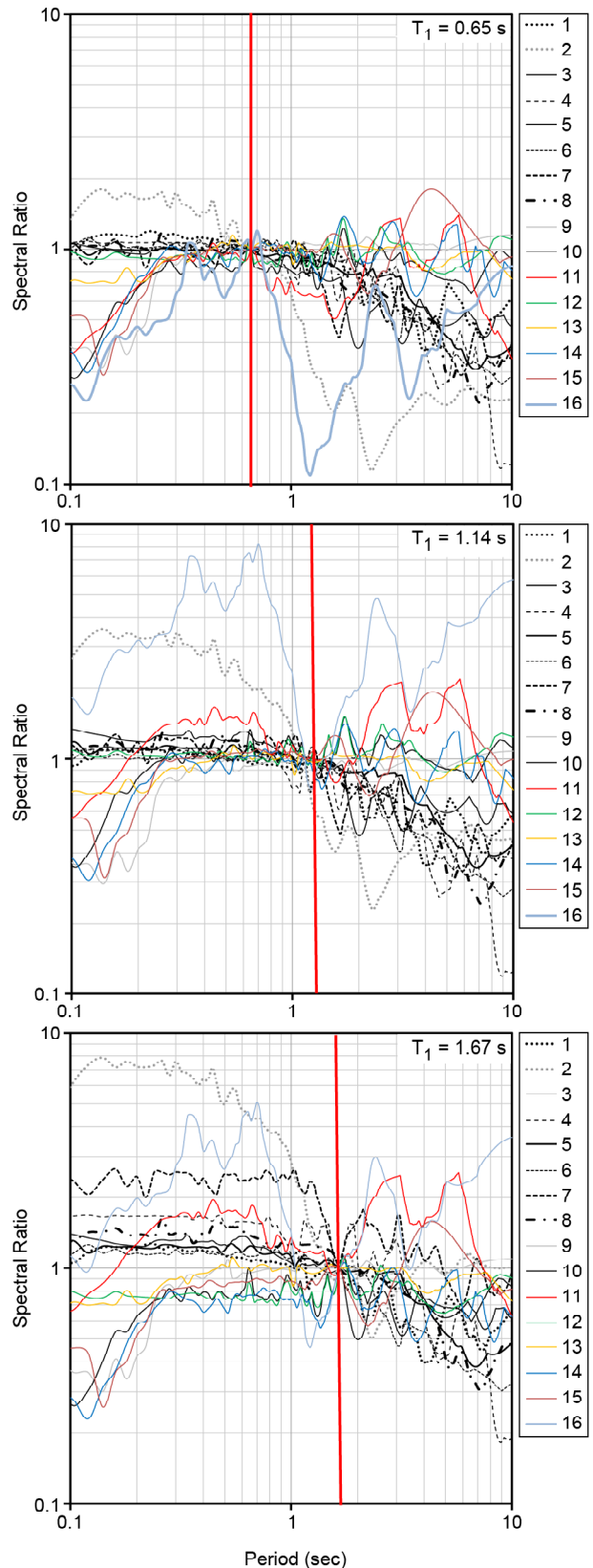**Figure 13.** Comparison of the mean IDA curves computed for the shortened and original records.



**Figure 14.** Spectral Ratios computed for different structural systems.

than $T_1$. The different observed trend is consistent with the output of IDA analysis, where IDA curve computed for ground motion No. 2 and No.16 deviate from exact prediction in all structural cases and even at the very small inter-story drift ratio (primitive elastic zone).

To trace the gradual deviation of the mean IDA curve in case of the mentioned ground motions for 6-story frame, Figure (15) is presented. Although, it can be concluded from this figure that some ground motions are main cause of observed difference between mean IDA curves and after omitting them the deviation is remarkably reduced, more extensive structural assessment is required to confirm the observed relationship between frequency content, spectral ratios and the predicted IDA curves.
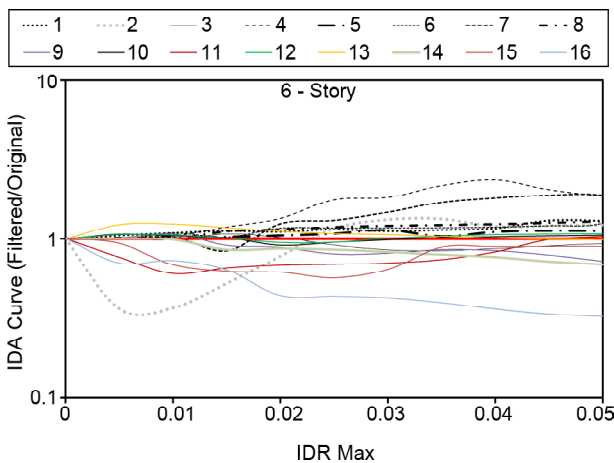


**Figure 15.** Gradual deviation from exact prediction of IDA curve spectral ratios computed for different structural systems.

## 6. Discussion

In this section, a quantitatively comparison between estimated seismic capacity of structures in terms of IDA results has been provided. Considering the drift ratio of 0.5, 2 and 4 percent as the corresponding the limit states for Immediate Occupancy, Life Safety and Collapse Prevention performance levels respectively. One can easily assess the efficiency of proposed method in application for probabilistic demand analysis of structures. The mention comparison has been made in case of mean, mean + standard deviation and mean - standard deviation.

For 3-story frame, there is a difference of 4.9%, 8.5% and 19.4% between two estimations of mean, mean + std (standard deviation) and mean - std IDA

curves, respectively at IO level. Also, there is a difference of 8%, 14% and 1.6% between two estimations of mean, mean + std and mean - std IDA curves, respectively at LS level. The observed difference is 9.8%, 12.1% and 5.9% in case of mean, mean + std and mean - std IDA curves, respectively at CP level.

In the case of 6-story frame, a difference of 5.1%, 0.2% and 12.2% between two estimations of mean, mean + std and mean - std deviation IDA curves has been observed, respectively at IO level. Furthermore, there is a difference of 9.7%, 15.3% and 3.1% in mean, mean + std and mean - std IDA curves, respectively at LS level. The mentioned difference is 1.9%, 1.7% and 2.5% at CP level.

For 12-story frame, a difference of 18.6%, 31.5% and 29.4% has been calculated between two estimations of mean, mean + std and mean - std IDA curves, respectively at IO level. Also, there is a difference of 16.2%, 24.2% and 27.9% between two estimations at LS level. Finally, the mentioned values of differences have been estimated as 0.2%, 3.35% and 12.9% between two estimations at CP level.

## 7. Conclusions

In this paper, after the introduction of S-Transform as a modern effective time-frequency representation, a new S-Transform-Based method was proposed to reduce the duration of Strong Ground Motion (SGM) excitation and, consequently the computational cost of NLTHA. Based on the numerical response calculations performed in this research the following conclusions can be made:

❖ The shortened SGMs can be an acceptable alternative for original accelerograms in term of Engineering Demand Parameters (EDPs) estimated by elastic analyses.

❖ It is observed that for nonlinear SDOF systems the use of shortened SGMs may cause non-negligible deviation in the estimated EDPs compared to the results obtained by using original SGMs. Considering the fact that the shortened SGMs as the result of proposed method in this paper are not scaled to have the same peak ground values of their corresponding original SGMs, such difference between the computed EDPs is expected.

❖ Based on the discussion presented in previous

item about the scaling, one can conclude that the application of an efficient scaling method before doing NLTHA can reduce the mentioned difference between the estimated EDPs.

❖ The estimations of the dynamic capacity of MDOF structures using IDA show the ability of the shortened SGMs to represent the original one in the generation of mean IDA curves. It should be noted that by a mean reduction of 71% in the duration of SGMs a difference of 9.8%, 1.9% and 0.2% is observed between the mean estimated collapse capacity of 3, 6 and 12-story frames, respectively.

❖ The possible error, which can be produced in the computed EDPs, due to the reduction of duration based on the proposed method can be assessed and predicted before NLTHA by comparing the elastic spectral response of shortened and original SGMs. Further research is needed in this regard.

## References

1. Wang, W. (1975) *Structural Instability during Earthquakes and Acceleration Simplification.* Ph.D. Theses, Michigan University, Ann Arbor, USA.

2. Iunio, I., Manfredi, G., and Cosenza, E. (2006) Ground motion duration effects on nonlinear seismic response. *Earthquake Engineering & Structural Dynamics*, **35**(1), 21-38.

3. Soroushian, A. (2008) A technique for time integration analysis with steps larger than the excitation steps. *Communications in Numerical Methods in Engineering*, **24**, 2087-2111.

4. Hosseini, M. and Mirzaei, I. (2013) Simplification of earthquake accelerograms for rapid time history analysis based on the impulsive load concept. *4th ECCOMAS Thematic Conference on Computational Methods in Structural Dynamics and Earthquake Engineering*, COMPDYN 2013.

5. Faroughi A. and Hosseini, M. (2011) Simplification of earthquake accelerograms for quick time history analyses by using their modified inverse fourier transforms. *Procedia Engineering*, **14**, 2872-2877.

6. Basim, M.Ch. and Estekanchi, H.E. (2015) Application of endurance time method in performance-based optimum design of structures. *Structural Safety*, **56**, 52-67.

7. Cheng, S., Xian, J., and Huang, H. (2021) An iterative equivalent linearization approach for stochastic sensitivity analysis of hysteretic systems under seismic excitations based on explicit time-domain method. *Computers and Structures*, **242**, 106396.

8. Soroushian, A. (2017) Integration step size and its adequate selection in analysis of structural systems against earthquakes. *Computational Methods in Earthquake Engineering*, Springer, Cham, 285-328.

9. Rathje, E.M., Abrahamson, N.A., and Bray, J.D. (1998) Simplified frequency content estimates of earthquake ground motions. *Journal of Geotechnical and Geoenvironmental Engineering*, **124**(2), 150-159.

10. Cakir, T. (2013) Evaluation of the effect of earthquake frequency content on seismic behavior of cantilever retaining wall including soil-structure interaction. *Soil Dynamics and Earthquake Engineering*, **45**, 96-111.

11. Salehi, R., Akbarpour, A., and Shalbaftabar, A. (2020) Fire Evaluation of RC Frames Strengthened with FRPs Using Finite Element Method. *American Journal of Engineering and Applied Sciences*, **13**(4), 610-626.

12. Reagan, C., Baker, J.W., and Deierlein, G.G. (2016) Quantifying the influence of ground motion duration on structural collapse capacity using spectrally equivalent records. *Earthquake Spectra*, **32**(2), 927-950.

13. Zhang, S., Wang, G., Pang, B., and Du, C. (2013) The effects of strong motion duration on the dynamic response and accumulated damage of concrete gravity dams. *Soil Dynamics and Earthquake Engineering*, **45**, 112-124.

14. Feng, H., Cui, X.Y., and Li, G.Y. (2016) A stable nodal integration method with strain gradient for static and dynamic analysis of solid mechanics. *Engineering Analysis with Boundary Elements*,

**62**, 78-92.

15. Du, J., Cui, C., Bao, H., and Qiu, Y. (2014) Dynamic analysis of cable-driven parallel manipulators using a variable length finite element. *ASME. J. Comput. Nonlinear Dynam.*, **10**(1), 011013.

16. Mukherjee, S. and Gupta, V.K. (2002) Wavelet-based characterization of design ground motions. *Earthquake Engng. Struct. Dyn.*, **31**, 1173-1190.

17. Gurley, K. and Kareem, A. (1999) Applications of wavelet transforms in earthquake, wind and ocean engineering. *Engineering Structures*, **21**, 149-167.

18. Qin, S.R. and Y.M., Zhong (2004) Research on the unified mathematical model for FT, STFT and WT and its applications. *Mechanical Systems and Signal Processing*, **18**(6), 1335-1347.

19. Bentley, P.M. and McDonnell, J.T.E. (1994) Wavelet transforms: an introduction. *Electronics and Communication Engineering Journal*, **6**(4), 175-186.

20. Stockwell, R.G., Mansinha, Lalu and Lowe, Robert (1996) Localisation of the complex spectrum: The S Transform. *IEEE Transaction on Digital Signal Processing*, **44**, 99-114.

21. Ghodrati Amiri, G. and S. Arian Moghaddam (2014) Extraction of forward-directivity velocity pulses using S-Transform-based signal decomposition technique. *Bulletin of Earthquake Engineering*, **12**(4), 1583-1614.

22. Hasan, Md Junayed and Kim, Jongmyon (2018) Bearing fault diagnosis under variable rotational speeds using atockwell transform-based vibration Imaging and transfer learning. *Applied Sciences*, **8**, 2357.

23. Bajaj, A. and Kumar, Sanjay (2019) QRS complex detection using fractional Stockwell transform and fractional Stockwell Shannon energy. *Biomedical Signal Processing and Control*, **54**, 101628.

24. Latfaoui, M. and Bereksi Reguig, F. (2018) Packets wavelets and stockwell transform analysis of femoral doppler ultrasound signals. *International Journal of Electrical and Computer Engineering*, (2088-8708), **8**(6).

25. Parolai, S. (2009) Denoising of seismograms using the S transform. *Bulletin of the Seismological Society of America*, **99**, 226-234.

26. Fan, J. and Dong, P. (2008) *Simulation of Artificial Near-Fault Ground Motions Based on the S-Transform*. Congress on Image and Signal Processing.

27. Ghodrati Amiri, G. and Arian Moghaddam, S. (2012) New method for generation of synthetic near-fault earthquake records based on S-transform. *15WCEE*, Lisbon.

28. Ditommaso, R., Mucciarelli, M., and Ponzo, F.C. (2012) Analysis of non-stationary structural systems by using a band-variable filter. *Bull Earthquake Eng.*, **10**, 895-911.

29. Ditommaso, R., Ponzo, F.C., and Auletta, G. (2015) Damage detection on framed structures: modal curvature evaluation using Stockwell Transform under seismic excitation. *Earthq. Eng. Eng. Vib.*, **14**, 265-274.

30. Shah, F.A. and Tantary, A.Y. (2020) Linear canonical Stockwell transform. *Journal of Mathematical Analysis and Applications*, **484**(1), 123673.

31. Ditommaso, R. et al. (2010) S-Transform based filter applied to the analysis of nonlinear dynamic behaviour of soil and buildings. *14th European Conference on Earthquake Engineering*, Ohrid, Republic of Macedonia.

32. Uang, C.-M. and Bertero, V.V. (1990) Evaluation of seismic energy in structures. *Earthquake Engng. Struct. Dyn.*, **19**, 77-90.

33. MathWorks, Inc. (2005) *MATLAB: the Language of Technical Computing*. Desktop Tools and Development Environment, Version 7. Vol. 9.

34. Mahin, S.A. and Lin, J. (1983) Construction of inelastic response spectra for single-degree-of-freedom systems. *Earthquake Engineering Center*, University of California, Berkeley.

35. Kamrava, A. (2015) *Comparing Results of MATLAB and Seismo Signal in Plotting Earthquake Graphs*. Current World Environment, **10**, Special Issue, 11.

36. Elnashai, A. and Di Sarno, L. (2008) *Fundamentals of Earthquake Engineering*. Wiley.

37. Mazzoni, Silvia, et al. (2006) *OpenSees Command Language Manual*. Pacific Earthquake Engineering Research (PEER) Center.

38. Karavasilis, T.L., Bazeos, N., and Beskos, D.E. (2008) Drift and ductility estimates in regular steel MRF subjected to ordinary ground motions: a design-oriented approach. *Earthquake Spectra*, **24**(2), 431-451.

39. Dimopoulos, A.I., Bazeos, N., and Beskos, D.E. (2012) Seismic yield displacements of plane moment resisting and x-braced steel frames. *Soil Dynamics and Earthquake Engineering*, **41**, 128-140.

40. Vamvatsikos, D. and Cornell, C.A. (2002) Incremental dynamic analysis. *Earthquake Engineering and Structural Dynamics*, **31**(3), 491-514.

41. ATC-63 (2008) *Quantification of Building Seismic Performance Factors ATC-63 Project Report-90% Draft*. Prepared by the Applied Technology Council for the Federal Emergency Management Agency.